Toward better genetically encoded sensors of membrane potential

Douglas Storace[1], Masoud Sepehri Rad[2], BokEum Kang[2], Lawrence B. Cohen[1,2], Thom Hughes[3], and Bradley J. Baker[2].

[1]Department of Cellular and Molecular Physiology, Yale University School of Medicine, New Haven, CT 06520, USA.

[2]Center for Functional Connectomics, Korea Institute of Science and Technology (KIST), Seoul, 136-791, Korea.

[3]Department of Cell Biology and Neuroscience, Montana State University, Bozeman, Montana 59717, USA.

Corresponding authors: Cohen, L. B. (lawrence.b.cohen@hotmail.com), Baker, B. J. (bradley.baker19@gmail.com)

Key words: genetically encoded voltage indicators, GEVIs, genetically encoded calcium indicators, GECIs, Ehud Isacoff, Thomas Knopfel

Running title: New and better GEVIs.

Abstract.

Genetically encoded sensors of cell activity are powerful tools that can be targeted to specific cell types. This is especially important in neuroscience because individual brain regions can include a multitude of different cell types. Understanding function will require recording activity from each of the individual cell types in a region. To this end, optical signals of membrane potential are useful because membrane potential changes are a direct sign of both synaptic and action potentials and because optical imaging allows for simultaneous recording from numerous neurons or brain regions. Here we describe recent improvements in the *in vitro* and *in vivo* signal size and kinetics of genetically encoded voltage indicators (GEVIs) and discuss their relationship to alternative sensors of neural activity.

Trends Box

- Recently developed genetically encoded voltage sensors (GEVIs) have larger and faster fluorescence signals.
- The new GEVIs result in improved signal-to-noise ratios in *in vivo* measurements in the mammalian brain.
- In some instances GEVI signals are substantially faster and more informative than measurements with genetically encoded calcium sensors (GECIs).

Rationale

Optical measurements of brain activity are attractive because they make it possible to simultaneously monitor activity from many individual neurons or from many different brain regions (population signals). In 1937 Sherrington[1] imagined points of light signaling the activity of nerve cells and their connections. During sleep only a few remote parts of the brain would twinkle. But at awakening, “Swiftly the head-mass becomes an enchanted loom where millions of flashing

shuttles weave a dissolving pattern." In the 80 years since this poetic description there have been significant advances towards making optical measurements of neural activity a reality. In this review we attempt to explain why GEVIs (see Glossary) would be useful and describe recent progress in developing improved sensors with larger and faster signals. We also compare GEVI signals with those from genetically encoded calcium indicators (GECIs).

GEVIs have been used *in vivo* for measurement of spike activity from individual cells and for measurement of population signals. With rare exceptions, [2] [3] most of the individual neuron recordings have been from invertebrates [4] [5] [6, 7] while population signals have been measured from mammalian preparations (e.g., [8, 9] [10] [11]). This review emphasizes recordings from mammalian preparations. Additionally we have attempted to restrict our discussion to those approaches to GEVI development that hold the greatest promise for the future. For earlier reviews of GEVIs see [12, 13, 14] .

The membrane potential changes of neuronal cells can vary dramatically from hyperpolarizations during neuronal inhibition to depolarizations from excitatory synaptic activity to the firing of action potentials. These different kinds of membrane potential change can complicate the interpretation of GEVI optical signals from populations of neurons especially in situations where different cell types have different kinds of activity. Restricting the response of a GEVI to one type of activity (*e.g.*, inhibition or action potentials) would facilitate the analysis of population signals. The voltage sensitivity of mosaic GEVIs (see below), with sigmoidal fluorescence vs voltage relationships, can be 'tuned' to respond to specific voltage ranges and thus report specific types of neuronal activity [15, 16] Measuring synaptic signals require a high dynamic range indicator but only low (> 10 ms) temporal resolution. In contrast action potentials can be measured with lower dynamic range but fast (< 1 ms) temporal resolution.

Beginning with Stosiek et al [17] , calcium signals have been used as a surrogate for a direct measure of action potentials on the assumptions that action potentials are the only source

of the measured calcium changes and that calcium changes occur during action potentials in all types of neurons. These assumptions are certainly not universally true [18, 19] but none-the-less calcium signals are widely used as indicators of spike activity. This is due to a combination of the large signal-to-noise ratios of genetically encoded calcium indicators (GECIs) and, until recently, the quite small signal-to-noise ratios of fluorescent protein voltage sensors (GEVIs). Furthermore, calcium changes and the resulting signals are much slower and thus are better suited to the frame rates available in 2-photon imaging. Recent reviews of calcium imaging and GECIs are available elsewhere [20, 21, 22]

Following a brief history of the development of GEVIs we describe the varieties of GEVI structures that have been explored. We then present examples of GEVI function in cultured HEK293 cells and neurons followed by an example of *in vivo* measurements. We present a table including one example GEVI from each of the laboratories developing GEVIs. We present evidence that a voltage sensitive monomer-dimer equilibrium may underlie the fluorescence change of some mosaic GEVIs. Lastly, we compare GEVIs with GECIs.

GEVI history.

The first human-made GEVI was a mosaic constructed by inserting an fluorescent protein (FP) into a voltage sensitive protein that resides in the plasma membrane. FlaSh, developed by Siegel and Isacoff [23] , was a voltage gated potassium channel with GFP inserted following the 6th transmembrane segment. Aside from its importance as a proof-of-principle, FlaSh had the useful feature of a steep, sigmoidal fluorescence vs voltage relationship that could, in principle, be tuned to select for different ranges of membrane potential. However, FlaSh also had drawbacks; its signal was relatively slow (tau ~100 msec), and small ($\Delta F/F$ <5%). But, most importantly, FlaSh, and the analogue Flare, worked in frog oocytes but not at all in mammalian cells. In mammalian cells, Flare's expression, and that of two other first generation GEVIs that were also based on mammalian ion channels, were mainly intracellular [24] . The Thomas

Knopfel laboratory overcame this obstacle by changing the membrane resident voltage sensor to the voltage sensitive domain of the *Ciona intestinalis* voltage sensitive phosphatase [15] . The first member of this family, VFSP2.1, expressed well in the plasma membrane of mammalian cells and had signals in response to changes in membrane potential. However, the *Ciona* voltage sensitive domain exhibits a gating current that lies far outside of the physiological voltage range [25] . The R217Q mutation shifted the voltage curve to a physiological range [15] but made the sensor slower [16] .

Schematic diagrams of GEVI types.

A number of recent GEVI developments have focused on mosaic proteins using the voltage sensitive domain of the *Ciona* voltage sensitive phosphatase as well as analogues from other vertebrate species. Three varieties of mosaic GEVIs are illustrated schematically in Figure 1A. The left panel illustrates a single fluorescent protein (FP) mosaic (example, ArcLight; [26]); the middle panel a mosaic with a “butterfly” FRET pair [27] of fluorescent proteins where the two FPs are on opposite sides of the voltage sensitive domain (example, Nabi2.244; [28]) and the right panel a mosaic with a circularly permuted fluorescent protein inserted in the external loop between transmembrane segments 3 and 4 (example, ASAP1; [29]).

A second type of GEVI utilizes the voltage sensitivity of microbial rhodopsins (Figure 1B; [30]). Both the absorption and fluorescence of the microbial rhodopsins are voltage sensitive but their fluorescence quantum efficiency is ~100 times smaller than GFP and thus GEVIs that are composed of the single microbial rhodopsin chromophore (left panel) require high intensity illumination to achieve an adequate fluorescence signal-to-noise ratio (example, Arch; [31]).

By combining the microbial rhodopsin in a mosaic with a second, bright, fluorescent protein (Figure 1B, right panel) a voltage sensitive FRET quenching signal is obtained (example MacQ-mCitrine; [2]). A third type of GEVI is a two component sensor that utilizes FRET quenching

between a membrane bound fluorescent protein and a charged membrane resident molecule as the voltage sensor (Figure 1C; example, hVOS; [32]). The voltage sensor, dipicrylamine, in hVOS has to be externally applied by the experimenter.

FRET-based GEVIs that are ratiometric (i.e. with two similarly bright FPs) have the advantage that the ratio removes common mode noise due to movement, e.g., respiration and blood flow, in an *in vivo* measurement. However the fluorescent intensities of the donor and acceptor FPs are often different, which means the shot noise of the ratio will be higher than that of either individual signal [33, 34] . FRET quenching signals are not ratiometric because there is only a single optical signal (from the fluorescent donor). In this review we have reported values of the fractional fluorescence change, ΔF/F; the fractional ratio change, ΔR/R, is only applicable to sensors with FRET signals.

Examples of GEVI signals in cultured HEK293 cells, in cultured neurons, and *in vivo*.

GEVI signals in HEK293 cells: example: ArcLight, a single FP mosaic protein [26] .

Serendipity resulted in ArcLight, a mosaic of the *Ciona* voltage sensitive domain and the GFP derivative, super ecliptic pHluorin [35] A227D. Figure 2A shows the location of A227. The black trace in Figure 2B shows the response to a 100 mV depolarization in a HEK293 cell using the native super ecliptic pHluorin. The red trace is the response with the spontaneous A227D mutation. This mutation increased the signal size by a factor of 15. The signal size was increased by another factor of 2 by shortening the linker between S4 and the fluorescent protein resulting in a fractional fluorescence change, ΔF/F, of ~40% per 100 mV (Figure 2C). This ΔF/F was five times larger than the previous largest [36, 37] GEVI signal.

Figure 2D is a plot of the ArcLight fluorescence signal vs membrane potential. The $V_{1/2}$ for the fluorescence change is -20 mV. Thus ArcLight will be maximally sensitive to membrane potentials that occur during action potentials but will still have some sensitivity to changes near

the resting potential. Other mutations to the voltage sensitive domain could make the GEVI more sensitive to synaptic potentials or to inhibition ([16]).

ArcLight's kinetics are not fast; the response to a step change in membrane potential is best fit by two components (see Figure 2B,C) with time constants of ~10 and ~50 msec at 33^{o}C. As a result, ArcLight signals during action potentials will not be as large as those found in response to longer voltage clamp steps [26] .

GEVI signals in cultured neurons: example QuasAr2; a single chromophore microbial rhodopsin [38] .

The kinetics of QuasAr2 are substantially faster than those of ArcLight. The QuasAr2 signal is also best fit by two exponentials with a fast time constant of 0.3 msec and a slow time constant of 3 msec at 34^{o}C. Because of its faster time constants, the QuasAr2 action potential signals are expected to more closely follow the time course of the action potential and the size of the action potential signal is expected to be closer to the size predicted by 100 msec voltage clamp steps. These expectations are confirmed by the QuasAr2 signal shown in Figure 3.

Even though the fluorescence quantum efficiency of QuasAr2 and other microbial rhodopsin single chromophore GEVIs is ~100 times smaller than that of ArcLight, the signal-to-noise ratio for the action potential recording in Figure 3 is large. This was achieved by using a high intensity incident light, 200Wcm^{-2}, about 100 times brighter than that used for GFP based GEVIs such as ArcLight. The dim fluorescence of single chromophore microbial rhodopsins is likely to limit their use *in vivo* mammalian preparations because the GEVI signal is likely to be submerged in the intrinsic tissue fluorescence and also because high intensity illumination is likely to damage the brain.

All of the microbial rhodopsin signals have a linear fluorescence vs membrane potential relationship [31, 38] and thus they cannot be tuned to detect specific kinds of potential changes.

GEVI signals *in vivo*: example ArcLight [11] .

The *in vivo* expression and function of GECIs and GEVIs has often been a challenge resulting in smaller than expected *in vivo* signal-to-noise ratios. AAV1 transduction was successfully used to express ArcLight in the mouse olfactory bulb. In the outer layers of the bulb the expression was specific for mitral/tufted neurons. Figure 4A illustrates a single trial, single glomerulus mitral/tufted response to an odorant stimulus that lasted for four inspirations. During each breath the ArcLight signal increased and then returned to the baseline. This measurement reflects the population average of the optical signals from the ~50 mitral/tufted cell dendrites in a glomerulus and is the expected result from action potential recordings from mitral/tufted cells which spike only during the inspiration phase [39] . Repeated trials gave similar results (Figure 4B) indicating that phototoxicity and photobleaching were minimal.

Box 1

Comparison of GEVIs and GECIs as indicators of neuron activity. Paired recordings of ArcLight and GCaMP3 in the same preparation in response to one and two inspirations of ethyl tiglate are shown in Figure 4C. A similar comparison of ArcLight and GCaMP6f is shown in Figure 4D. The longer odor presentations resulted in breath coupled responses that were very obvious with ArcLight, but relatively small with both GCaMPs. These are population signals; both ArcLight and the GCaMPs are in the glomerular dendrites of ~50 mitral/tufted cells which innervate each glomerulus.

Although ArcLight had a smaller ΔF/F and signal-to-noise ratio than the GCaMPs, its signal was large enough to report odor-evoked signals in response to a single inspiration in single trials in individual glomeruli. ArcLight had a faster onset, rise time, and decay than the GCaMPs and could track the odor-evoked signal across successive inspirations of an odor[11] . In contrast, the GCaMP measurements were saturating integrals of the odor-evoked neural activity.

Because action potentials sometimes cause large influxes of calcium mediated by voltage-gated calcium channels [40] [41] , calcium dyes and GECIs are commonly used as surrogates for voltage dyes and GEVIs in detecting action potentials in individual mammalian neurons. Calcium sensors have the important advantage of larger signal-to-noise ratio.

However, voltage-gated calcium channels are not the only source of calcium entry in a cell, and thus calcium signals do not always reflect spike activity. Subthreshold depolarizations elicited clear calcium transients in mitral cells [18] . Calcium influx can also occur through ligand-gated receptors [42] [22] and can be further modulated by release from internal stores of calcium [43, 44, 45] . Furthermore, action potentials generate little or no calcium influx in some cell types [19] .

Calcium dynamics are also slow in contrast with voltage changes which blurs the relationship between the optical signal and spike rates except at very low rates [41, 46, 47] . Optical measurements from protein calcium sensors can be further confounded by nonlinearities with respect to calcium concentration [21] , and by the kinetics of the protein sensor [11, 48] . GECIs are also likely to miss hyperpolarizations in neurons with low rates of spontaneous spiking, whereas some GEVIs can be tuned to respond differentially to hyperpolarization or depolarization [16, 49] .

ArcLight's ability to report odor-evoked activity in single trials demonstrates that GEVIs can be a useful tool for *in vivo* measurements. That said, GEVIs and GECIs are complementary tools, where the appropriate use depends on whether the improved temporal resolution and membrane potential sensitivity of ArcLight is more important than the improved signal-to-noise ratio and calcium sensitivity of the GCaMPs.

Mechanisms responsible for one single FP mosaic GEVI signal.

The development of better GEVIs may be facilitated by determining the mechanism(s) that couple changes in membrane potential to changes in fluorescence. FRET-based constructs are superficially easy to understand: movements of the voltage sensing domain change the distance and/or orientation of the donor and acceptor chromophores resulting in a change in FRET. The fluorescence changes of probes with circularly permuted FPs such as ASAP-1 and Electric-PK are also theoretically straightforward by saying that movement of S4 alters the β-barrel structure. However, an explanation for the optical signal from mosaic GEVIs which consist of a single FP residing in the cytoplasm is not obvious. How does the movement of the S4 transmembrane domain cause a fluorescent signal from a cytoplasmic FP? The results presented below suggests a surprising hypothesis.

Because super ecliptic pHluorin is pH sensitive, a possible mechanism for the fluorescence change involves pH. Only super ecliptic pHluorin was able to give large optical signals when the A227D mutation was present. The A227D mutant does not improve the optical signal for other FPs such as Clover, eGFP, or YFP. Recently, Han et al [50] obtained large signals from eGFP by introducing the A227D mutation along with three other mutations found in super ecliptic pHluorin. These mutations converted eGFP into a pH-sensitive FP suggesting that these GEVIs might be measuring pH. However, a single mutation that increased the pH sensitivity did not result in a large signal [50] . Furthermore, Kang and Baker [51] measured a voltage-dependent optical signal and a pH-dependent signal simultaneously using the voltage-sensing domain of a voltage-gated proton channel fused to super ecliptic pHluorin A227D. A 200 mV depolarization resulted in the activation of the voltage-gated proton current which slowly decreased the internal pH of the cell resulting in a slow increase in fluorescence. A 100 mV depolarization did not activate the proton channel and only a voltage-dependent change in fluorescence was observed. Increasing the buffering capacity of the internal patch solution inhibited the pH-dependent fluorescence change but had no effect on the voltage-dependent

signal. These observations strengthen the conclusion that ArcLight and related analogues are not sensing membrane potential via a change in pH.

Hints for a different mechanism were first suggested during the development of ArcLight. The effect of the A227D mutation in this FP was remarkable. Surprisingly, A227D resides on the outside of the β-barrel structure suggesting that this mutation does not directly interact with the chromophore. Another hint was that the signal could be improved by optimizing the length of the amino acid linker between the cytoplasmic FP and the S4 transmembrane domain ([26, 50] . Both the linker length and the amino acid composition at the fusion site of the FP and the linker affected the optical signal, suggesting that the orientation of the FP was important [49] . These results led to the hypothesis that the super ecliptic pHluorin in ArcLight is dimerizing with the FP from an adjacent ArcLight protein. The movement of S4 then alters that interaction resulting in the change in fluorescence.

There are three mutations to eGFP that favor the monomeric version of the FP, A206K, L221K and F223R [52] . The GEVI TM [16] , an analogue of ArcLight, with 206A-221L-223F which favor dimerization has the largest signal (Figure 5, orange trace). Individual mutations favoring the monomer at the three sites reduced the signal; double mutations cause a further reduction (Figure 5). These data strongly support the hypothesis that movement of the S4 domain alters the dimerization interaction resulting in the change in fluorescence.

Reporting important characteristics for GEVIs.

A substantial list of characteristics determine the utility of a GEVI for monitoring brain activity. We discuss how well each of these characteristics are described in the literature and make suggestions about improving the description. Signal size (ΔF/F per 100 mv), kinetics (ms), and $V_{1/2}$ of fluorescence vs voltage (for GEVIs with sigmoidal responses) are routinely reported for measurements in cultured cells (often HEK293 cells). The characteristics below are often reported but usually only qualitatively.

Brightness. The brightness of an FP is the product of two factors, the extinction coefficient (ε) and the quantum yield (Φ). Quantum yield is simply the fraction of absorbed photons that lead to emitted fluorescence, while the extinction coefficient describes how strongly the chromophore absorbs light. For example, the fluorescent protein Clover has an extinction coefficient of 111,000 $M^{-1} cm^{-1}$ and quantum yield of 0.76 [53] making it one of the brightest fluorescent proteins. Brightness could be routinely reported.

Expression level. A measurement of the average total fluorescence of a cell is an indication of expression level. For comparison purposes, this measurement should be corrected for brightness. Because the measurement of fluorescence will depend on characteristics of the measuring apparatus, an absolute value of expression level will be difficult to determine. However it would be easy to compare the expression level of a new GEVI with that of an already established GEVI.

Plasma membrane localization. All of the images of GEVI expression that we are aware of have substantial intracellular expression. This intracellular expression will reduce the signal-to-noise ratio. Two different methods have been used to measure plasma membrane localization. First, Figure 3 of Baker et al [24] illustrates a measurement of plasma membrane expression using confocal microscopy. The GEVI fluorescence is compared to an externally added dye which binds to but does not cross the plasma membrane. Second, Bedbrook et al [54] used an extracellular tag in a SpyTag/SpyCatcher system to measure the plasma membrane localization of channelrhodopsin. This scheme might also work for GEVIs.

Signal-to-noise ratio. This critical GEVI characteristic is not easily absolutely quantified because of its dependence on the preparation and the measurement apparatus. But a comparison with a previously established GEVI would be relatively easy and very useful.

Steepness of fluorescence vs voltage (for GEVIs with sigmoidal responses). This characteristic will determine how well a GEVI could distinguish between action potentials,

excitatory synaptic potentials, and inhibitory synaptic potentials. Fluorescence vs voltage curves are typically fit with the Boltzmann equation, $Y = (A_1 - A_2)/(1 + e^{(V - V_{1/2})/dx}) + A_2$, where A_1 is the minimum value, and A_2 is the maximum value and dx is the slope (steepness) of the Boltzmann fit. The slope should be routinely reported.

***In vivo* characterization**. *In vivo* measurement of these characteristics is clearly important. First, because the *in vivo* result may be different from the *in vitro* result and second, because *in vivo* characterization will inform scientists who are deciding which, if any, GEVI to use. *In vivo* measurement of some characteristics will be difficult because they require simultaneous fluorescence and patch clamp measurements.

ArcLight could be a standard. It has a decent ΔF/F and seems to work well *in vivo* [11] . ArcLight is freely available from many sources; it is available for worms and transgenic *Drosophila* and several AAV viruses successfully transfect rodent brains. Lastly, it has already been used in several comparisons.

GEVI recording of spike activity in individual neurons in the mammalian brain.

Because of light scattering by the tissue, 2-photon microscopy is needed to image individual neurons in the *in vivo* brain. Using a frame rate of 100 Hz, Storace et al [11] measured 2-photon population signals from populations of mitral/tufted cell dendrites in response to odorant presentation from individual glomeruli in the mouse olfactory bulb. However, optimal recording of individual spikes from individual mammalian cells *in vivo* requires a frame rate of 1000 Hz which will limit the 2-photon recording to line scans or narrow rectangles. Results from this kind of measurement have not yet been reported. Peron et al, [20] called attention to the anticipated difficulties. A GEVI with a fast onset but slow offset would reduce the requirement for fast frame rates.

Concluding Remarks

Developing improved GEVIs is both unpredictable and challenging yet success seems likely. Several results (e.g. Figures 2 and 5, [15]) have shown that changing individual amino acids in either the voltage sensitive domain or in the fluorescent protein of a mosaic GEVI can have dramatic effects on performance. Similarly, the location of the FP in the voltage sensitive domain also has dramatic effects on GEVI function [28, 29] . Improving GEVIs involves investigations in a very large multi-parameter space. Furthermore, it is not often that a planned mutation in a GEVI has the planned result. The situation is further complicated by the fact that many different characteristics of the GEVI are important for its functionality. As a result high-throughput methods for improving GEVIs have thus far concentrated on individual characteristics (e.g. brightness [38]).

At the same time, the opportunities for improving GEVIs are also very large because investigation of the multi-parameter space is only just beginning and, as Figure 1 and Table 1 indicate, many approaches are under active investigation. In addition, Kang et al [55] provide evidence that an unanticipated dimerization mechanism is responsible for some single FP mosaic GEVI signals. This finding is likely to guide further attempts at improvement of mosaic GEVIs.

Future development is needed in two new directions. First, to provide better GEVIs with red signals so that simultaneous measurements could be made from two cell types or simultaneous stimulation and recordings could be carried out in the same brain region. Second, to target GEVIs to specific regions of the neuron so that the optical signal could be specific for nerve terminals, or dendrites, or the soma. This would improve the signal-to-noise ratio in many kinds of measurements.

Outstanding Questions.

- Can GEVIs be useful in monitoring the spike activity of many individual cells in the mammalian brain? While spike signals from an individual cell have been detected using

signal averaging, this use of GEVIs poses challenges. Mammalian action potentials are very fast (width <2 msec) and thus obtaining the optimal signal-to-noise ratio requires frame rates of ~1 kfps. Except for line scans these rates are difficult to achieve using 2-photon microscopy (which is necessary for imaging individual cells in the mammalian brain). Clearly, improved GEVIs (faster, larger signals) will be important for this application.

- What is the mechanism responsible for the GEVI fluorescence change? The results presented in Figure 5 suggest that voltage affects the equilibrium between monomers and dimers of that GEVI. Will this conclusion be true of other mosaic GEVIs? Will this information lead to the development of better GEVIs?
- Can red shifted GEVIs with large signals be developed? Red sensors would allow simultaneous recordings from two cells types. Red sensors also have the advantage of reduced scattering of red wavelengths by the brain.

Acknowledgements

Supported by US NIH grants DC005259 and NS054270, grant number WCI 2009-003 from the National Research Foundation of Korea, a James Hudson Brown – Alexander Brown Coxe fellowship from Yale University, and a Ruth L. Kirschstein National Research Service Award DC012981.

Table 1. Properties of selected GEVIs

	ΔF/F for a 100 mV depolarization (HEK293 cells)	Fast ON tau (100 mV depolarization (ms)	Single trial signals in neurons	Single trial *in vivo* signals	Comments	References
mosaic single FP GEVIs						
ArcLight	40%	10	yes	yes		[4, 11, 26]
Bongwoori	20%	8	yes	not tested		[16]
ASAP1	17%	2	yes	not tested		[29]
Arclightning	10%	10	not tested	not tested	much faster OFF tau	[56]
mosaic butterfly GEVIs						
Nabi2.213	11%	3	yes	not tested	PC12 cells	[28]
VSFP-Butterfly 1.2	4%	2	not tested	yes		[27]
Mermaid2	20%	2	yes	yes		[9]
microbial-rhodopsin GEVIs					linear F vs V	
Archer1	80%	2	yes	yes	small QE, cultured neurons; *C. elegans*	[5]
QuasAr2	90%	<<1	yes	not tested	small QE	[38]
MacQ-mCitrine	20%	5	yes	yes	mosaic	[2]
two component GEVIs						
nVOS	30%	0.5	yes	not tested	PC12 cells; linear F vs v	[32, 57]

Glossary

FP: a fluorescent protein (e.g. Green Fluorescent Protein (GFP))

FRET: fluorescence resonance energy transfer. Transfer of energy from one FP to a second, neighboring, FP

GEVI: genetically encoded voltage indicator

GECI: genetically encoded calcium indicator

S1-S4: numbering of transmembrane helices in the voltage sensitive domain of the *Ciona* phosphatase.

super ecliptic pHluorin: A pH sensitive variation of GFP.

Figure Legends.

Figure 1. Schematic structures of three types of GEVIs. **(A)**. Mosaic sensors combining the voltage sensitive domain of a voltage sensitive phosphatase and a fluorescent protein. **(B)**. Sensors based on the voltage sensitivity of a microbial rhodopsin. **(C)**. Sensors that are a combination of two separate molecules. Figure 1B was modified from [58]). Figure 1C was modified from Wang et al, [32]

Figure 2. Characterization of ArcLight, a single FP mosaic sensor. **(A)**. The location of the outward facing A227 amino acid. **(B)**. The A227D mutation increased the signal size by a factor of 15. **(C)**. A further increase in signal was found if the linker between the S4 segment and the FP was shortened. **(D)**. The fluorescence change vs membrane potential was sigmoidal with a $V_{1/2}$ of -20 mV. Modified from [26] .

Figure 3. A simultaneous optical and electrode measurement of an action potential in a cultured hippocampal neuron using the microbial rhodopsin GEVI QuasAr2. Modified from [58] .

Figure 4. *In vivo* measurements using ArcLight, a single FP mosaic GEVI. The mitral/tufted cells were transduced by infection with an AAV1 virus containing ArcLight DNA. **(A)**. A single trial, single glomerulus measurement of the response to the odorant ethyl tiglate presented during four breaths. **(B)**. The overlay of the responses to six repeated trials. There was little change from trial to trial. **(C)**. Comparing ArcLight and GCaMP3 signals from opposite olfactory bulbs in the same preparation in response to odorant presentations lasting one and two breaths. **(D)**. Comparing ArcLight and GCaMP6f. Modified from [11] .

Figure 5. The effect of monomeric mutations at the dimerization site of a single FP mosaic GEVI. **A**. The GEVI TM with 206A-221L-223F which favor dimerization has the largest signal (orange). Individual mutations favoring the monomer at the three sites reduced the signal; double mutations cause a further reduction. **B**. A schematic model of a TM dimer. Modified from [55] .

References

1. Sherrington, S.c. (1937) *Man on His Nature*. Cambridge University Press.
2. Gong, Y., Wagner, M.J., Zhong Li, J., and Schnitzer, M.J. (2014) Imaging neural spiking in brain tissue using FRET-opsin protein voltage sensors. *Nature communications* 5, 3674.
3. Akemann, W., Mutoh, H., Perron, A., Rossier, J., and Knöpfel, T. (2010) Imaging brain electric signals with genetically targeted voltage-sensitive fluorescent proteins. *Nature Methods* 7, 643-649.
4. Cao, G., Platisa, J., Pieribone, V.A., Raccuglia, D., Kunst, M., and Nitabach, M.N. (2013) Genetically targeted optical electrophysiology in intact neural circuits. *Cell* 154, 904-913.
5. Flytzanis, N.C., Bedbrook, C.N., Chiu, H., Engqvist, M.K., Xiao, C., Chan, K.Y., . . . Gradinaru, V. (2014) Archaerhodopsin variants with enhanced voltage-sensitive fluorescence in mammalian and Caenorhabditis elegans neurons. *Nature communications* 5, 4894.
6. Kunst, M., Hughes, M.E., Raccuglia, D., Felix, M., Li, M., Barnett, G., . . . Nitabach, M.N. (2014) Calcitonin gene-related peptide neurons mediate sleep-specific circadian output in Drosophila. *Current biology : CB* 24, 2652-2664.
7. Klein, M., Afonso, B., Vonner, A.J., Hernandez-Nunez, L., Berck, M., Tabone, C.J., . . . Samuel, A.D. (2015) Sensory determinants of behavioral dynamics in Drosophila thermotaxis. *Proceedings of the National Academy of Sciences of the United States of America* 112, E220-229.
8. Akemann, W., Sasaki, M., Mutoh, H., Imamura, T., Honkura, N., and Knopfel, T. (2013) Two-photon voltage imaging using a genetically encoded voltage indicator. *Scientific reports* 3, 2231.
9. Tsutsui, H., Jinno, Y., Tomita, A., Niino, Y., Yamada, Y., Mikoshiba, K., . . . Okamura, Y. (2013) Improved detection of electrical activity with a voltage probe based on a voltage-sensing phosphatase. *J Physiol* 591, 4427-4437.
10. Mishina, Y., Mutoh, H., Song, C., and Knopfel, T. (2014) Exploration of genetically encoded voltage indicators based on a chimeric voltage sensing domain. *Frontiers in molecular neuroscience* 7, 78.
11. Storace, D.A., Braubach, O.R., Jin, L., Cohen, L.B., and Sung, U. (2015) Monitoring brain activity with protein voltage and calcium sensors. *Scientific reports* 5, 10212.
12. St-Pierre, F., Chavarha, M., and Lin, M.Z. (2015) Designs and sensing mechanisms of genetically encoded fluorescent voltage indicators. *Current opinion in chemical biology* 27, 31-38.
13. Storace, D., Rad, M.S., Han, Z., Jin, L., Cohen, L.B., Hughes, T., . . . Sung, U. (2015) Genetically Encoded Protein Sensors of Membrane Potential. *Advances in experimental medicine and biology* 859, 493-509.
14. Knopfel, T., Gallero-Salas, Y., and Song, C. (2015) Genetically encoded voltage indicators for large scale cortical imaging come of age. *Current opinion in chemical biology* 27, 75-83.
15. Dimitrov, D., He, Y., Mutoh, H., Baker, B.J., Cohen, L., Akemann, W., and Knopfel, T. (2007) Engineering and characterization of an enhanced fluorescent protein voltage sensor. *PLoS One* 2, e440.
16. Piao, H.H., Rajakumar, D., Kang, B.E., Kim, E.H., and Baker, B.J. (2015) Combinatorial mutagenesis of the voltage-sensing domain enables the optical resolution of action potentials firing at 60 Hz by a genetically encoded fluorescent sensor of membrane potential. *The Journal of neuroscience : the official journal of the Society for Neuroscience* 35, 372-385.

17. Stosiek, C., Garaschuk, O., Holthoff, K., and Konnerth, A. (2003) In vivo two-photon calcium imaging of neuronal networks. *Proceedings of the National Academy of Sciences of the United States of America* 100, 7319-7324.
18. Charpak, S., Mertz, J., Beaurepaire, E., Moreaux, L., and Delaney, K. (2001) Odor-evoked calcium signals in dendrites of rat mitral cells. *Proceedings of the National Academy of Sciences of the United States of America* 98, 1230-1234.
19. Helmchen, F., Svoboda, K., Denk, W., and Tank, D.W. (1999) In vivo dendritic calcium dynamics in deep-layer cortical pyramidal neurons. *Nature neuroscience* 2, 989-996.
20. Peron, S., Chen, T.W., and Svoboda, K. (2015) Comprehensive imaging of cortical networks. *Current opinion in neurobiology* 32, 115-123.
21. Rose, T., Goltstein, P.M., Portugues, R., and Griesbeck, O. (2014) Putting a finishing touch on GECIs. *Frontiers in molecular neuroscience* 7, 88.
22. Ross, W.N. (2012) Understanding calcium waves and sparks in central neurons. *Nature reviews. Neuroscience* 13, 157-168.
23. Siegel, M.S. and Isacoff, E.Y. (1997) A genetically encoded optical probe of membrane voltage. *Neuron* 19, 735-741.
24. Baker, B.J., Lee, H., Pieribone, V.A., Cohen, L.B., Isacoff, E.Y., Knopfel, T., and Kosmidis, E.K. (2007) Three fluorescent protein voltage sensors exhibit low plasma membrane expression in mammalian cells. *Journal of neuroscience methods* 161, 32-38.
25. Murata, Y., Iwasaki, H., Sasaki, M., Inaba, K., and Okamura, Y. (2005) Phosphoinositide phosphatase activity coupled to an intrinsic voltage sensor. *Nature* 435, 1239-1243.
26. Jin, L., Han, Z., Platisa, J., Wooltorton, J.R., Cohen, L.B., and Pieribone, V.A. (2012) Single action potentials and subthreshold electrical events imaged in neurons with a fluorescent protein voltage probe. *Neuron* 75, 779-785.
27. Akemann, W., Mutoh, H., Perron, A., Park, Y.K., Iwamoto, Y., and Knopfel, T. (2012) Imaging neural circuit dynamics with a voltage-sensitive fluorescent protein. *Journal of neurophysiology* 108, 2323-2337.
28. Sung, U., Sepehri Rad, M., Jin, L., Hughes, T., Cohen, L.B., and Baker, B.J. (2015) Improving signal dynamics of fluorescent protein voltage sensors by optimizing FRET interactions. *PLoS ONE* in press

29. St-Pierre, F., Marshall, J.D., Yang, Y., Gong, Y., Schnitzer, M.J., and Lin, M.Z. (2014) High-fidelity optical reporting of neuronal electrical activity with an ultrafast fluorescent voltage sensor. *Nature neuroscience* 17, 884-889.
30. Junge, W. and Witt, H.T. (1968) On the ion transport system of photosynthesis--investigations on a molecular level. *Zeitschrift fur Naturforschung. Teil B: Chemie, Biochemie, Biophysik, Biologie* 23, 244-254.
31. Kralj, J.M., Douglass, A.D., Hochbaum, D.R., Maclaurin, D., and Cohen, A.E. (2012) Optical recording of action potentials in mammalian neurons using a microbial rhodopsin. *Nat Methods* 9, 90-95.
32. Wang, D., Zhang, Z., Chanda, B., and Jackson, M.B. (2010) Improved probes for hybrid voltage sensor imaging. *Biophys J* 99, 2355-2365.
33. Wilt, B.A., Fitzgerald, J.E., and Schnitzer, M.J. (2013) Photon shot noise limits on optical detection of neuronal spikes and estimation of spike timing. *Biophys J* 104, 51-62.
34. Lee, S., Piao, H., Sepheri Rad, M., Jung, A., Sung, U., Song, Y.K., and Baker, B.J. (2015) Imaging membrane potential with two types of genetically encoded fluorescent voltage sensors *Journal of Visualized Experiments.* in press.
35. Miesenbock, G., De Angelis, D.A., and Rothman, J.E. (1998) Visualizing secretion and synaptic transmission with pH-sensitive green fluorescent proteins. *Nature* 394, 192-195.

36. Mutoh, H., Perron, A., Dimitrov, D., Iwamoto, Y., Akemann, W., Chudakov, D.M., and Knopfel, T. (2009) Spectrally-resolved response properties of the three most advanced FRET based fluorescent protein voltage probes. *PLoS One* 4, e4555.
37. Perron, A., Mutoh, H., Akemann, W., Gautam, S.G., Dimitrov, D., Iwamoto, Y., and T., K. (2009) Second and third generation voltage-sensitive fluorescent proteins for monitoring membrane potential. *Frontiers in molecular neuroscience* 2, doi: 10.3389/neuro.3302.3005.2009.
38. Hochbaum, D.R., Zhao, Y., Farhi, S.L., Klapoetke, N., Werley, C.A., Kapoor, V., . . . Cohen, A.E. (2014) All-optical electrophysiology in mammalian neurons using engineered microbial rhodopsins. *Nat Methods* 11, 825-833.
39. Rinberg, D., Koulakov, A., and Gelperin, A. (2006) Sparse odor coding in awake behaving mice. *The Journal of neuroscience : the official journal of the Society for Neuroscience* 26, 8857-8865.
40. Jaffe, D.B., Johnston, D., Lasser-Ross, N., Lisman, J.E., Miyakawa, H., and Ross, W.N. (1992) The spread of Na+ spikes determines the pattern of dendritic Ca2+ entry into hippocampal neurons. *Nature* 357, 244-246.
41. Callaway, J.C. and Ross, W.N. (1995) Frequency-dependent propagation of sodium action potentials in dendrites of hippocampal CA1 pyramidal neurons. *Journal of neurophysiology* 74, 1395-1403.
42. Schiller, J., Major, G., Koester, H.J., and Schiller, Y. (2000) NMDA spikes in basal dendrites of cortical pyramidal neurons. *Nature* 404, 285-289.
43. Emptage, N., Bliss, T.V., and Fine, A. (1999) Single synaptic events evoke NMDA receptor-mediated release of calcium from internal stores in hippocampal dendritic spines. *Neuron* 22, 115-124.
44. Garaschuk, O., Yaari, Y., and Konnerth, A. (1997) Release and sequestration of calcium by ryanodine-sensitive stores in rat hippocampal neurones. *J Physiol* 502 (Pt 1), 13-30.
45. Pozzo Miller, L.D., Petrozzino, J.J., Golarai, G., and Connor, J.A. (1996) Ca2+ release from intracellular stores induced by afferent stimulation of CA3 pyramidal neurons in hippocampal slices. *Journal of neurophysiology* 76, 554-562.
46. Markram, H., Helm, P.J., and Sakmann, B. (1995) Dendritic calcium transients evoked by single back-propagating action potentials in rat neocortical pyramidal neurons. *J Physiol* 485 (Pt 1), 1-20.
47. Svoboda, K., Denk, W., Kleinfeld, D., and Tank, D.W. (1997) In vivo dendritic calcium dynamics in neocortical pyramidal neurons. *Nature* 385, 161-165.
48. Wachowiak, M., Economo, M.N., Diaz-Quesada, M., Brunert, D., Wesson, D.W., White, J.A., and Rothermel, M. (2013) Optical dissection of odor information processing in vivo using GCaMPs expressed in specified cell types of the olfactory bulb. *The Journal of neuroscience : the official journal of the Society for Neuroscience* 33, 5285-5300.
49. Jung, A., Garcia, J.E., Kim, E., Yoon, B.J., and Baker, B.J. (2015) Linker length and fusion site composition improve the optical signal of genetically encoded fluorescent voltage sensors. *Neurophotonics* 2, 021012.
50. Han, Z., Jin, L., Chen, F., Loturco, J.J., Cohen, L.B., Bondar, A., . . . Pieribone, V.A. (2014) Mechanistic studies of the genetically encoded fluorescent protein voltage probe ArcLight. *PLoS One* 9, e113873.
51. Kang, B. and Baker, B.J. (2015) Pado, a fluorescent protein that resolves pH and membrane potential changes reveals insights into the voltage-dependent, optical signal. *submitted*.
52. Zacharias, D.A., Violin, J.D., Newton, A.C., and Tsien, R.Y. (2002) Partitioning of lipid-modified monomeric GFPs into membrane microdomains of live cells. *Science (New York, N.Y.)* 296, 913-916.

53. Lam, A.J., St-Pierre, F., Gong, Y., Marshall, J.D., Cranfill, P.J., Baird, M.A., . . . Lin, M.Z. (2012) Improving FRET dynamic range with bright green and red fluorescent proteins. *Nat Methods* 9, 1005-1012.
54. Bedbrook, C.N., Kato, M., Ravindra Kumar, S., Lakshmanan, A., Nath, R.D., Sun, F., . . . Gradinaru, V. (2015) Genetically Encoded Spy Peptide Fusion System to Detect Plasma Membrane-Localized Proteins In Vivo. *Chemistry & biology* 22, 1108-1121.
55. Kang, B. and Baker, B.J. (2015) Monomeric fluorescent proteins reduce the optical signal of genetically encoded voltage indicators. *submitted*.
56. Treger, J.S., Priest, M.F., and Bezanilla, F. (2015) Single-molecule fluorimetry and gating currents inspire an improved optical voltage indicator. *in press*.
57. Wang, D., McMahon, S., Zhang, Z., and Jackson, M.B. (2012) Hybrid voltage sensor imaging of electrical activity from neurons in hippocampal slices from transgenic mice. *Journal of neurophysiology* 108, 3147-3160.
58. Zou, P., Zhao, Y., Douglass, A.D., Hochbaum, D.R., Brinks, D., Werley, C.A., . . . Cohen, A.E. (2014) Bright and fast multicoloured voltage reporters via electrochromic FRET. *Nature communications* 5, 4625.

Figure 1

Schematic structures of three types of GEVIs

(A) Type 1:

voltage sensitive phosphatase based mosaic sensors

single FP

butterfly FRET pair

circularly permuted

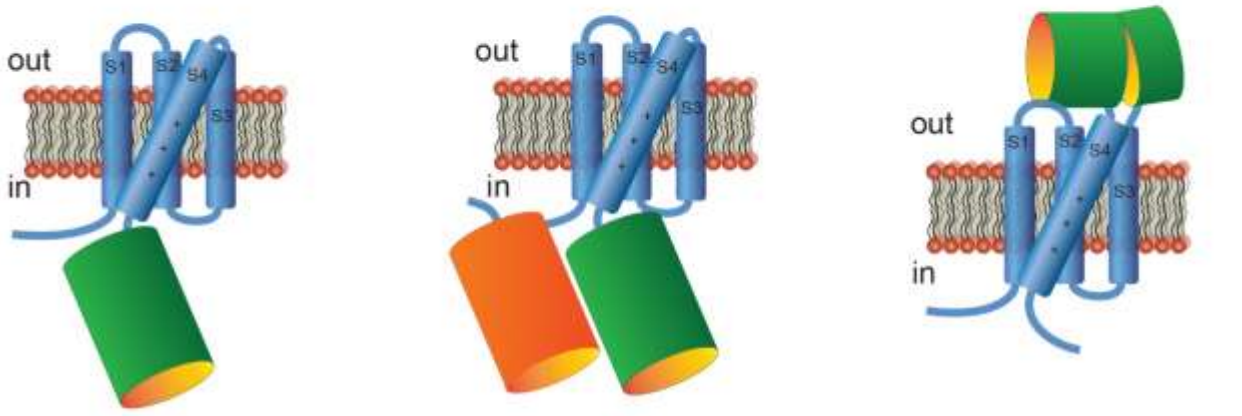

(B) Type 2:

microbial rhodopsin based sensors

single chromophore

FRET quenching

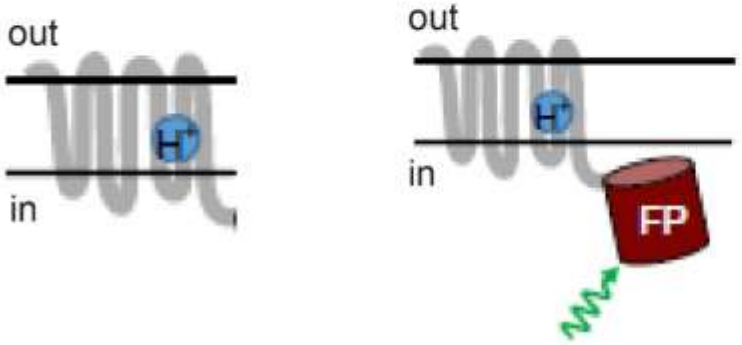

(C) Type 3:

dual component sensors

FRET quenching

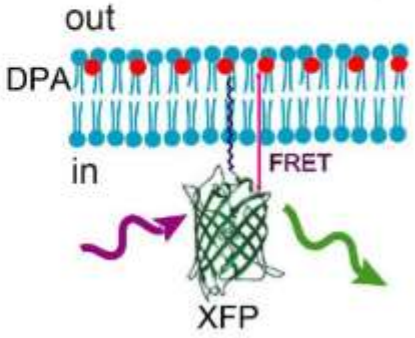

TiNS Figure 1.ai

Figure 2
Characterization of the GEVI, ArcLight

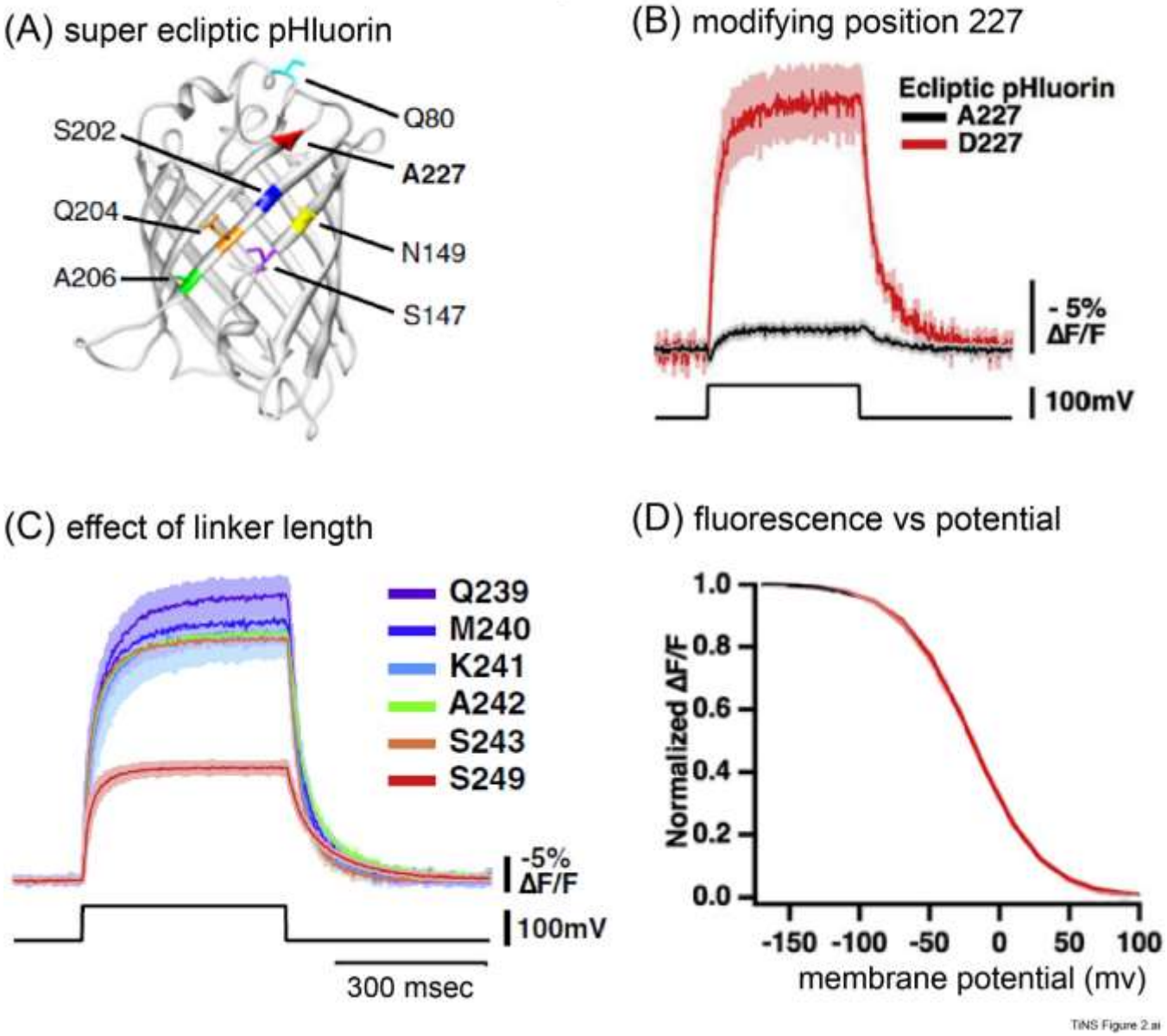

Figure 3

Action potential recording in a hippocampal neuron using QuasAR2.

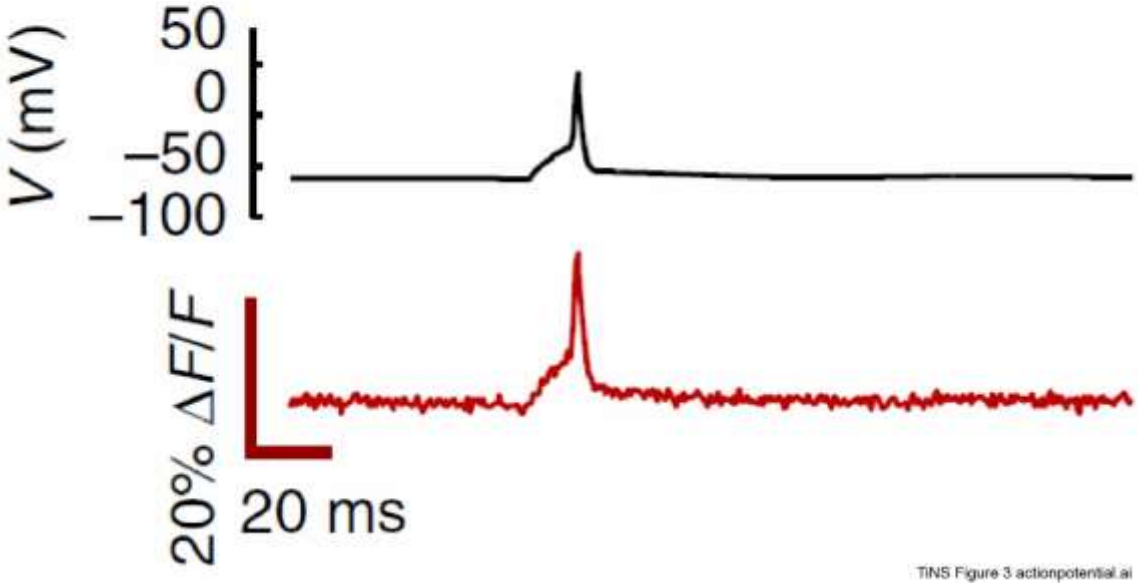

Figure 4

In vivo measurements; comparing GEVIs and GECIs

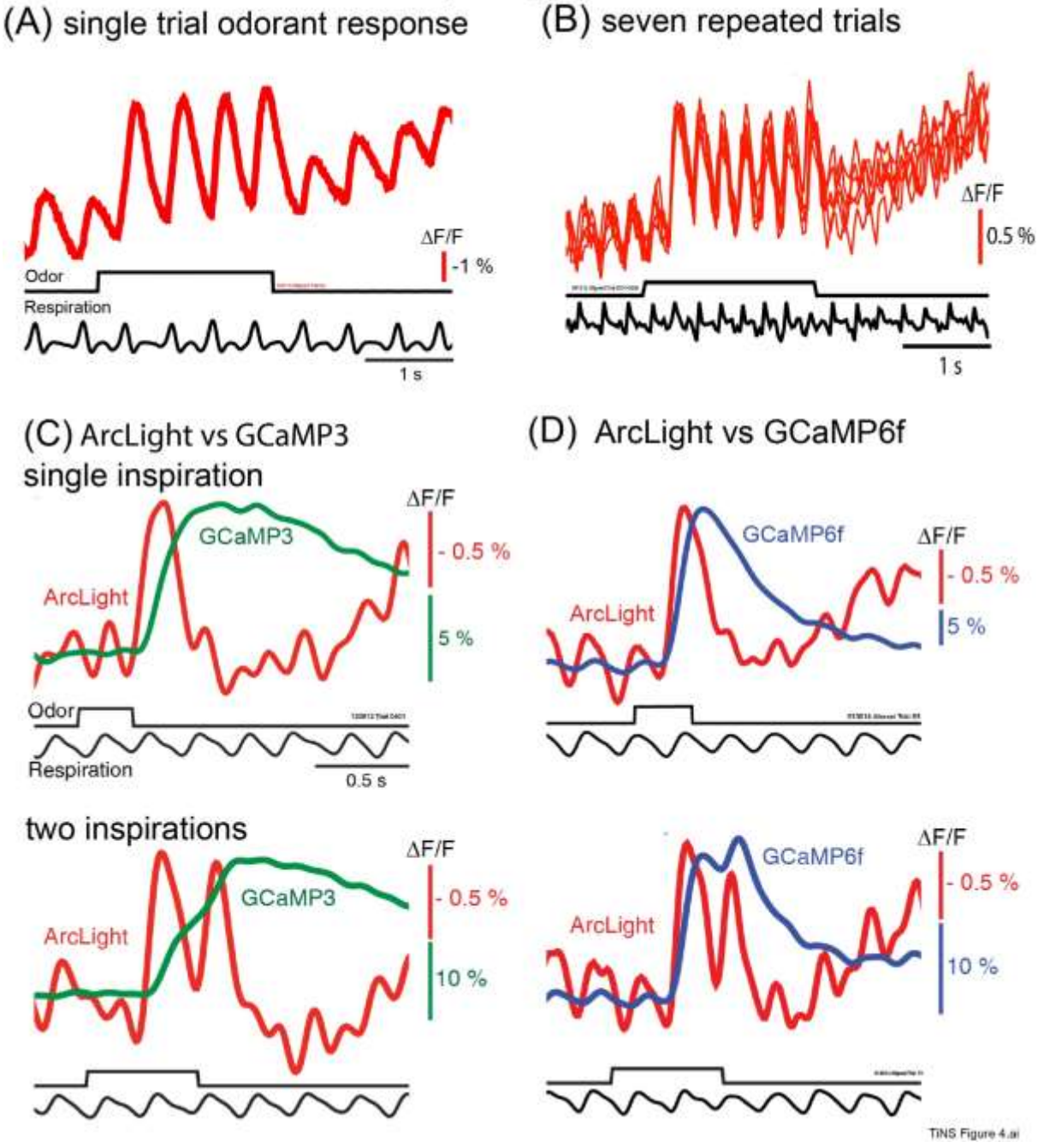

Figure 5

Effect of monomeric mutations at the dimerization interface

(A).

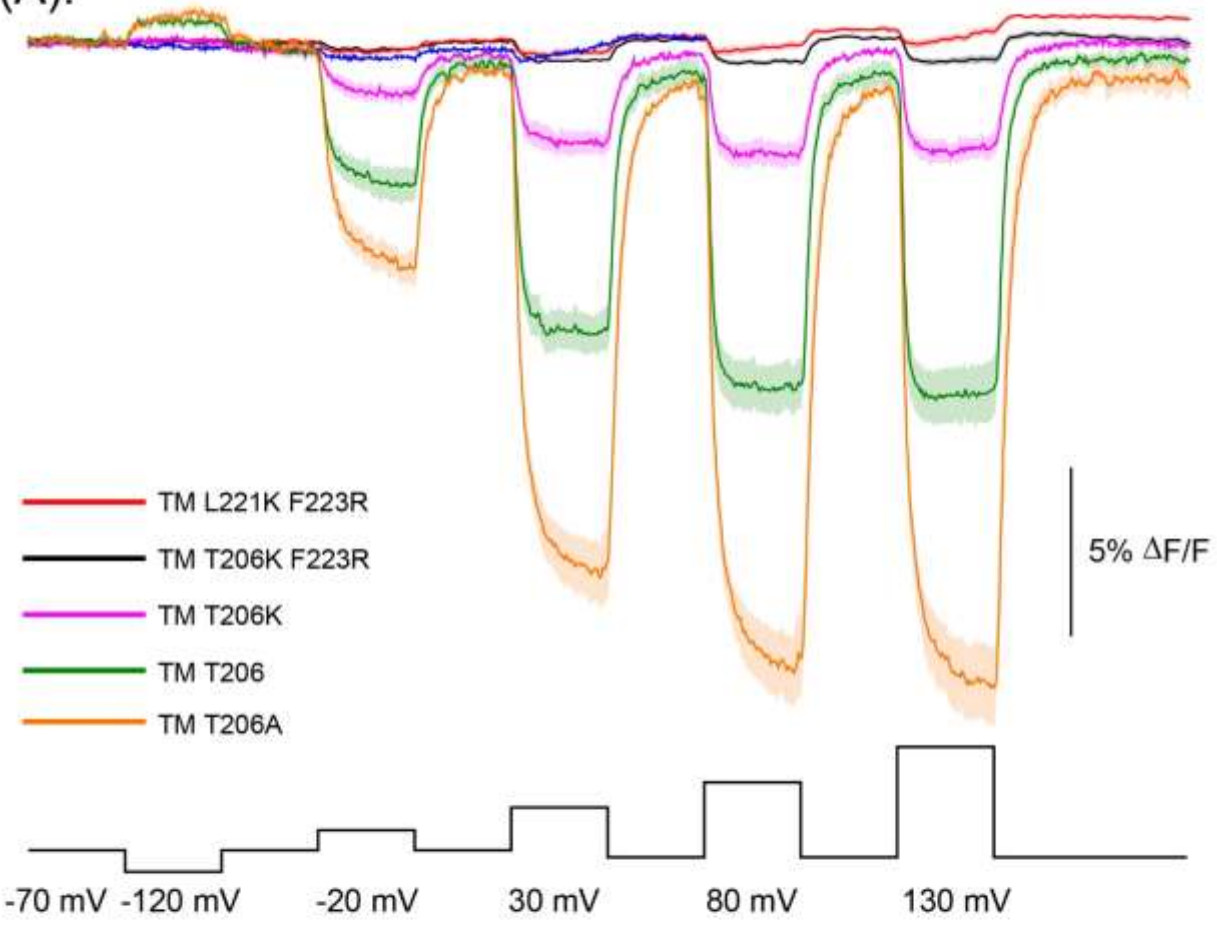

(B).

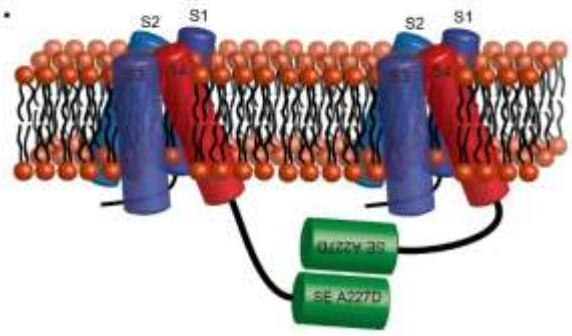

TiN5 Figure 5 dimer v2.ai